


Spectroscopy of high-pressure rubidium–noble-gas mixturesTill Ockenfels,^{*} Paško Roje[✉], Thilo vom Hövel[✉], Frank Vewinger[✉], and Martin Weitz
Institut für Angewandte Physik der Universität Bonn, Wegelerstrasse 8, D-53115 Bonn, Germany (Received 25 March 2022; accepted 21 June 2022; published 19 July 2022)

Spectroscopy of alkali-metal–buffer-gas mixtures at high pressures from single-digit to several hundred bars in the regime of substantial collisional broadening is relevant in a wide range of fields, ranging from collisional redistribution cooling to laboratory astrophysics. Here we report on spectroscopic measurements of dense rubidium–noble-gas mixtures recorded in a pressure cell equipped with soldered sapphire optical viewports, which allows for the controlled realization of extreme conditions of high temperature and high pressure in a table top laboratory experiment. In the gas cell, we have recorded absorption and emission spectra of rubidium subject to 188 bars of helium buffer-gas pressure at 548-K temperature. The spectra to good accuracy follow a Boltzmann-type Kennard-Stepanov frequency scaling of the ratio of absorption and emission spectral profiles. Further, the long optical path length in the cell allowed us to both record spectra of rubidium–argon mixtures at moderate temperatures and high pressures and observe redistributional laser cooling in this system.

DOI: [10.1103/PhysRevA.106.012815](https://doi.org/10.1103/PhysRevA.106.012815)**I. INTRODUCTION**

One of the most well-proven tools for the scientific investigation of both the composition of matter and the mechanisms determining its behavior on a microscopic level is optical spectroscopy. Over time this technique enabled the analysis of matter benefiting from the immense precision of this method. Additionally, it allows also to extract parameters of complex systems, such as temperature. In astronomy as well as in plasma physics optical spectroscopy is used as it is one of the tools to investigate the extreme conditions that the materials are exposed to, while they are out of reach for other methods of probing [1–3].

In gaseous systems, when, e.g., an atom approaches another atom, the energy levels are shifted due to the interaction, leading to a transient variation of the atom’s transition frequency. On the one hand, for frequencies close to resonance with a detuning below the inverse collisional duration, the impact limit is fulfilled, and provided that the collisions are elastic a symmetric line broadening occurs, accompanied by a linear shift of the line center. On the other hand, in the spectral wings, which become especially pronounced at higher pressures due to the increased overall broadening of the line, the impact limit does not hold anymore and the lines often become asymmetric, and show a nonlinear shift with increasing pressure. A precise knowledge of the molecular potential curves is then important for a prediction of the line shape, e.g., in the quasistatic approximation. When using inert gases as a buffer gas, the quenching of optical transitions is weak, and atoms in their electronically excited state undergo a large number of collisions (see, e.g., Refs. [4–7] for earlier work on the optical spectroscopy of dense alkali-metal–noble-gas mixtures). Especially the effect of a high-pressure environment

of the lightest noble gas helium acting as a buffer gas on the spectra of other elements is of great interest in astronomy as it is the second-most abundant element and represents 24% of the total baryonic mass in the universe [8].

In this paper we investigate absorption and emission spectra of rubidium–helium mixtures at a pressure of up to 188 bars and a temperature of 548 K in a table top laboratory experiment. The experiments benefit from using our proprietary high-pressure cell equipped with soldered sapphire optical viewports, where the sapphire is bonded to a metal flange via active soldering making use of a compound intermediate structure allowing one to mitigate thermally induced stress [9]. In the high-density environment the frequent collisions lead to a thermalization of the occupation distribution in the ground-state and excited-state manifolds. This has a number of well-known consequences for the spectral profiles: the Stokes shift and Kasha’s rule [10–13], which to a certain extent are clearly present in our measured spectra. Additionally, the assumption of a thermalization in the occupation of the excited-state manifold can be tested by verifying the Kennard-Stepanov relation [14,15] which is a Boltzmann-type scaling of the ratio of absorption and emission spectral profiles with frequency, and is known to be fulfilled in a wide range of systems like semiconductor quantum wells, doped glasses, photoactive biomolecules, dyes, and other mixtures of alkali metals and noble gases [5,6,16–21].

We report the measurement of rubidium absorption and emission spectra in the presence of high-pressure helium–buffer gas. The emission spectra were recorded making use of nonresonant laser excitation, while the absorption spectra were derived from a combination of standard absorption measurements with a scaled excitation spectrum as described in more detail in the following. In these spectra not only the pressure broadening and shift of the resonances known as the rubidium D_1 and D_2 lines are clearly visible but also strong signatures of satellite resonances the origin of which can

^{*}ockenfels@iap.uni-bonn.de

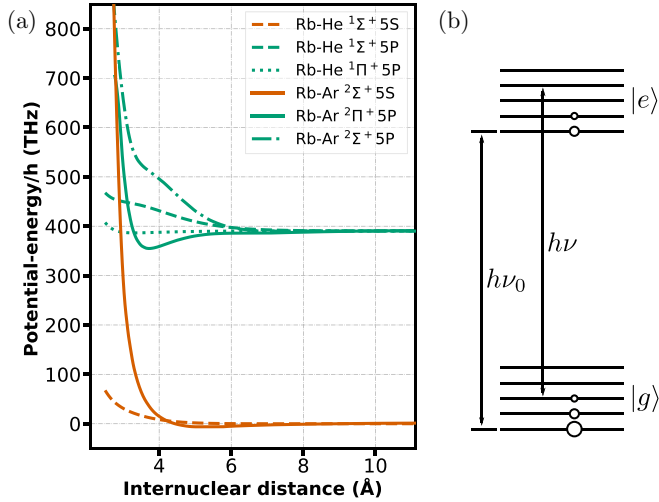


FIG. 1. (a) Potential-energy curves of the relevant first levels of Rb-He and Rb-Ar quasimolecules [30,31]. (b) Schematic Jablonski diagram of a two-level system with a sublevel structure in both the electronic ground and the excited states. The size of the dots is chosen so as to indicate thermal occupation in both the upper and lower electronic state.

be found in the form of the quasimolecular potential curves of the collisional partners. Further it can be shown that the ratio between absorption and emission spectral profiles well follows a Kennard-Stepanov frequency scaling over a wide frequency range, however the spectral temperature extracted from the logarithmic ratio is above the cell temperature. Additionally, results on redistributive laser cooling carried out at comparable parameters but in a rubidium-argon mixture are reported.

II. MODEL AND THEORY

In a binary-collisional picture, the effect of the interaction of atoms is described by potential curves as depicted in Fig. 1(a), showing the particle energy levels in relation to the distance to a collision partner [22–24]. These potentials allow for theoretical predictions of the expected spectra via calculations, e.g., based on the Franck-Condon principle when the atomic motion is so slow with respect to the collisional time that the quasistatic approximation applies [25,26]. The frequency range of the absorbed or emitted photons of a certain electronic transition is then determined by the energy differences of the potential curves, and to calculate a spectral profile weighting factors are taken into account for the relative probability of an electronic transition taking place while the perturber is at a specific distance to the atom under consideration. The quasistatic approximation is capable of predicting the shape of spectral profiles away from the resonances as well as distinct satellite resonances resulting from the form of the potential curves for a given pressure and temperature [27]. We point out that for more accurate line-shape predictions united line broadening theories are commonly used, e.g., the Anderson-Talman method [28,29].

Upon increased pressure, frequent collisions can furthermore lead to thermalization within the quasimolecular

manifolds of electronic levels. For a noble-buffer-gas pressure in the 100-bar range, collisions occur on a 10^{-11} -s timescale, which is far faster than the upper electronic state lifetime of D -line transitions of alkali-metal atoms. In this limit, a Boltzmann-like Kennard-Stepanov scaling between absorption and emission spectral profiles has been observed in rubidium-argon-buffer-gas mixtures [5,6].

Following a model developed by Sawicki and Knox [17] originally in the context of the description of dye spectra, the Kennard-Stepanov relation can straightforwardly be derived for a two-level system with a ground state $|g\rangle$ and an excited state $|e\rangle$, each with an additional sublevel structure. For a long enough lifetime of the electronically excited state to allow for the sublevel structure to acquire thermal equilibrium in the presence of coupling to the thermal environment, the occupation of the sublevels in ground and excited manifolds will follow a Boltzmann distribution, as depicted in Fig. 1(b). By making use of the Einstein A-B relation and the energy conservation, the ratio between the absorption $\alpha(\nu)$ and the emission spectra $f(\nu)$ is found to be [17]

$$\frac{f(\nu)}{\alpha(\nu)} \propto \exp\left(\frac{-h(\nu - \nu_0)}{k_B T}\right) \frac{8\pi\nu^3}{c^2}. \quad (1)$$

In the limit of the quasistatic approximation, the same result has also been derived using a standard collisional theory model [5]. Thermalization in electronic submanifolds here means that detailed balance applies to both the bound and free eigenstates of the quasimolecular manifolds. For small detunings ($\nu - \nu_0 \ll \nu_0$) the free space mode density $\frac{8\pi\nu^3}{c^2}$ can be assumed to be constant and formula Eq. (1) can be rewritten to

$$\ln\left(\frac{\alpha(\nu)}{f(\nu)}\right) = \frac{h}{k_B T}\nu + D(T), \quad (2)$$

which shows the known linear scaling of the logarithmic ratio of the absorption and emission profile with the optical frequency.

Another consequence that follows from the relaxation within the upper electronic state manifold is the fact that the form of the emission spectrum is independent of the excitation frequency, known as Kasha's rule. We point out that this redistribution of fluorescence is also essential for redistributive laser cooling [32], as will be discussed later.

III. METHODS AND SETUP

As mentioned above, under conditions of high pressure and high temperature the shape of observed spectral profiles tends to differ significantly from the spectra observed in undisturbed systems, which makes the observation of such spectra a suitable method to investigate the conditions in these systems in a contactless way. The experiments reported in this paper have been carried out in a high-pressure- and high-temperature-resistant gas cell construction recently realized by our group, providing a very reliable spectroscopic environment at these conditions. The cell is made from high-temperature stainless steel (1.4841) the openings of which are enclosed by flanges which house active-soldered sapphire windows providing optical access [9]. For preparation, this cell is first baked out at around 720 K to remove contaminations. It is then filled with

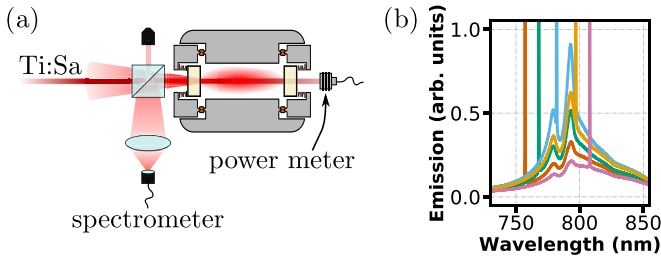


FIG. 2. (a) Optical setup for the detection of the emission from the gas mixture in a cell with one optical axis. The wavelength-tunable excitation laser beam is coupled into the cell through a polarizing beam splitter (PBS) where it excites atoms in the gas. The part of the resulting emission leaving the cell through the entrance window and reflected by the PBS is focused into a fiber coupler and sent to the spectrometer. (b) Emission spectra of the rubidium-helium mixture recorded for different excitation frequencies. As the shape of the spectral profile of the quasimolecular emission is always the same, Kasha's rule is well fulfilled.

1 g of high-purity rubidium, together with high-purity helium gas. In this filled cell we can bring the rubidium-noble-gas mixture to temperatures of up to 650 K and noble-gas pressures of up to 300 bars.

Figure 2(a) shows the setup we used to record the emission spectra of the gas mixture. We make use of a tunable titanium-sapphire laser, providing an optical power above 1 W in the wavelength range from 715 to 950 nm. With this laser we excite the system close to the rubidium D lines. Emitted fluorescence from the gas sample transmitted back through the entrance window and redirected by a beam splitter cube is focused into a multimode fiber attached to an optical spectrometer. We record spectra at different excitation wavelengths [see Fig. 2(b)], and the observed spectral signals, apart from showing scattered excitation beam light around the excitation wavelength, clearly follow Kasha's rule. Correspondingly, we combine multiple spectra at different excitation wavelengths to obtain emission spectra without residual excitation light.

Absorption spectra of the dense gas mixture are recorded by determining the variation of the fluorescence yield detected in backwards direction as a function of laser wavelength, which in the case of redistribution can well be assumed to be proportional to the absorption [6]. This yields raw data as in Fig. 2(b); note the visible variation of the line area for different incident laser wavelengths—the latter can be read off from the peak caused by scattered excitation light. To find the absorption coefficient we scale the data obtained from the wavelength dependence of the integrated fluorescence (naturally excluding the peak caused by scattered laser light) by overlapping them with data measured far from resonance at low optical density, where one can determine the absorption coefficient by directly comparing incident and transmitted beam power.

To test for an induced temperature change in the gas mixture due to redistributional laser cooling we use the method of deflection spectroscopy, where a position-dependent deflection of a second, nonresonant laser beam is recorded. From

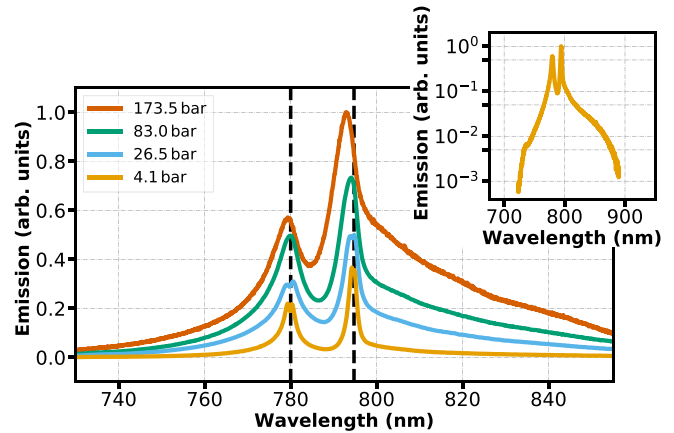


FIG. 3. Emission spectra from the rubidium-helium-gas mixture measured at a cell temperature of 507 K and different pressures. The two vertical dashed lines mark the position of the undisturbed D_1 and D_2 resonances. A pressure-dependent broadening and blueshift is visible. Inset: The emission spectrum at 4.1 bars shown in logarithmic scale for better comparison with the data in Refs. [38,39].

this deflection profile the temperature profile in the cell can be determined via contactless probing.

IV. RESULTS OF RUBIDIUM-HELIUM-GAS MIXTURE SPECTROSCOPY

In Fig. 3 emission spectra of rubidium-helium mixtures are shown recorded at a gas cell temperature of 507 K and a wide range of pressures from 4.1 to 173.5 bars. The rubidium density is assumed to be vapor limited, at a partial pressure of 0.22 mbar at this temperature. One sees strong broadening of the D_1 and D_2 resonances with pressure. Also, a pressure shift of both emission maxima from the position of the undisturbed resonances is clearly visible. The mean shift can be extracted from the spectra via a Lorentzian fit to the maxima to be (4.82 ± 0.07) GHz/bar for the D_1 line and (2.01 ± 0.12) GHz/bar for the D_2 line, respectively. For the D_1 transition this is around 40% larger than the literature values as they are presented in Table I, however we want to point out that the here determined shift of the emission line can differ from the shift of the absorption line, especially in light of the thermal redistribution present at high pressures. Also earlier work on emission spectra [33] gives different line shifts compared to those for absorption profiles.

For the D_2 line a much smaller pressure shift has been reported in earlier work; however, in a different pressure range, only the measurement at the highest pressure so far by Ch'en also shows a relatively strong shift of the D_2 line. We attribute this significant difference to the other literature values, mainly to the high pressures used in the presented work, where the assumption of a purely linear shift with pressure is not valid, as, e.g., a thermalization within the electronically excited D -line quasimolecular rovibrational manifolds occurs. Evidence for the thermalization present for the observed spectra is the relative line strength of the D_1 and D_2 lines, which is altered from a 1 : 2 ratio expected from the multiplicity, e.g., observed in the low-pressure regime, while here the lower energetic D_1 line emission is favored.

TABLE I. Overview of pressure-induced shifts of absorption and emission lines of the rubidium principal series reported previously and in this paper.

Publication	Year	P_{\max} (bars)	T (K)	D_1 shift (GHz/bar)		D_2 shift (GHz/bar)	
				Absorption	Emission	Absorption	Emission
Ch'en [34]	1940	101	580	3.33		1.34	
Ottinger <i>et al.</i> [33]	1974	1.5	318				0.52
Romalis <i>et al.</i> [35]	1997	13	353	3.3		0.35	
Rotondaro and Perram [36]	1997	0.4	394	3.62		0.28	
Miller <i>et al.</i> [37]	2016	20	343	3.54		0.15	
This paper		173	507		4.82		2.01

In the inset in Fig. 3 the emission spectrum of the rubidium-helium mixture recorded for the lowest pressure of 4.1 bars is shown again in logarithmic scale. In this visualization one sees that the form of the spectrum away from the resonance is not the same for red and blue detuning. Red detuned from the resonances the emission strength drops off relatively slowly and for wavelengths higher than 865 nm the slope changes and a shoulderlike feature arises. For blue detuning the emission decreases much faster, yet around 735 nm an additional feature in the form of a satellite resonance is visible. In the literature predicted spectra for this system at slightly different parameters (temperature of 1000 K and a density of $1 \times 10^{20} \text{ cm}^{-3}$, equating to around 14 bars at that temperature) can be found [38,39]. When comparing the general form of the emission spectra they are nevertheless in good agreement. The shape of the red wing with its changing slope is present in the calculated spectra as well as the satellite peak at blue detuning.

In Fig. 4(a) measured absorption as well as emission spectra of the rubidium-helium system are shown for a pressure of 188 bars. The use of such high pressures well ensures a full redistribution of fluorescence, as is necessary to apply the above described method (see Sec. III) of extracting the absorption strength from the detected fluorescence yield, as this method relies heavily on the spectral profile of the emission being independent of the excitation frequency. The absorption

shows a smooth decline in the absorption strength red detuned to the resonances while in the blue wing a satellite resonance at 865 nm is visible, which becomes visible at the same position in the calculated spectra in Ref. [38] for temperatures of 320 K and larger. This satellite is of certain interest for the realization of exciplex-pumped alkali-metal-gas lasers [40].

To verify the before claimed fulfillment of the Kennard-Stepanov relation in Fig. 4(b) the natural logarithm of the ratio of the absorption and emission spectra is shown. This ratio is in very good agreement with the plotted linear function over a large range of 100 nm, which equates to $5.9 k_B T$ [compare formula Eq. (2)]. Small discrepancies between the logarithmic ratio and the linear fit can be seen at the positions of the resonances, which is attributed to the maxima not being fully resolved due to technical limitations. Also for a large red detuning from the resonances the emission signal shows a satellite peak where there is no additional feature in the absorption spectrum, which leads to a disturbance in the logarithmic ratio. The slope of the fitted function corresponds to a spectral temperature of 812 K, which is above the cell temperature of 548 K. The discrepancy is most probably either due to an incomplete thermalization of the upper electronic state quasimolecular manifold at the used pressure for the light helium buffer gas or a finite quantum yield of the system in the presence of this noble gas. To investigate the origin of the incomplete thermalization in more detail, time-resolved spectroscopy could be carried out in future. In earlier work of our group studying mixtures of alkali metals with the heavier argon noble gas, the spectral temperature was in very good agreement with the cell temperature [6,41].

V. RESULTS OF RUBIDIUM-ARGON-GAS MIXTURE SPECTROSCOPY

While the optical path length of 100 mm of the cell described here is obstructive when trying to resolve the maximum absorption strength on resonance it yet enables measurements on gas mixtures of relatively low temperature resulting in little rubidium evaporation and therefore relatively small rubidium densities of $7 \times 10^{10} \text{ cm}^{-3}$, corresponding to a partial pressure of 0.5 mbar. In Fig. 5(a) emission and absorption spectra of a rubidium-argon mixture at a temperature of 530 K and 131 bars of total pressure are shown. Due to the full redistribution of the fluorescence the form of the emission spectrum here to good accuracy is not dependent on the excitation frequency. In comparison with earlier publications [5,6] these measurements were carried out at significantly different

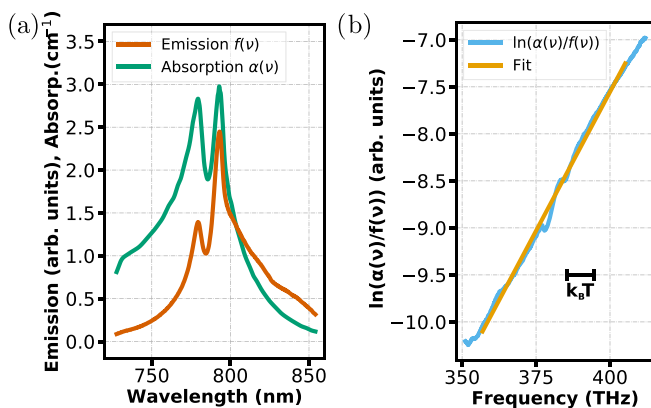


FIG. 4. (a) Emission and absorption spectra of the Rb-He mixture measured at 548 K and 188 bars (in comparison to Fig. 3 a higher temperature was chosen to be able to observe the satellite resonance). (b) The natural logarithm of the ratio of the spectral profiles vs the optical frequency.

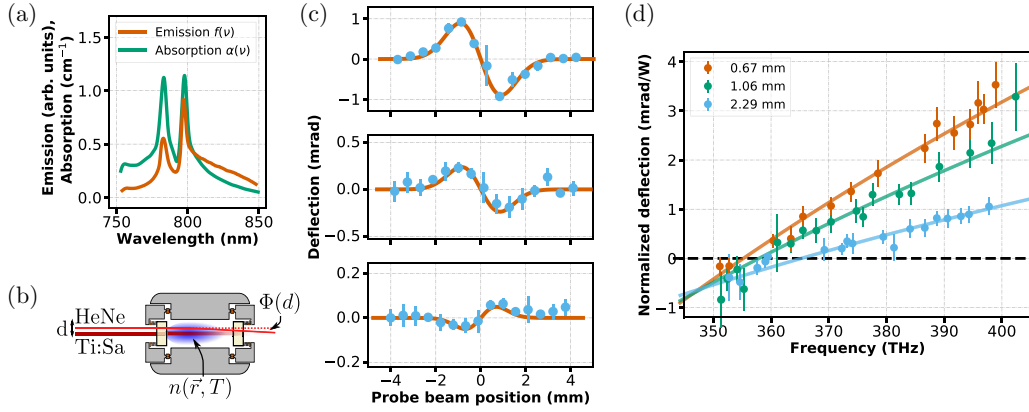


FIG. 5. (a) Emission and absorption spectra of the Rb-Ar mixture measured at 530 K and 131 bars. (b) Sketch of the used optical setup for measurements of the temperature-induced deflection of the probe beam. (c) Individual deflection signals at three different cooling beam frequencies [402.3 THz (745.0 nm), 365.4 THz (820.2 nm), and 352.6 THz (849.8 nm)]. The orientation being flipped for the most red-detuned excitation indicates cooling of the gas. Recorded with a beam diameter of the cooling laser of 1.06 mm. (d) Normalized deflection measurements for different cooling beam diameters together with fitted functions.

cell temperatures and pressures, respectively, which results in altered spectral profiles.

Further, the greater optical path length also allows for a sufficient interaction between the photons from the excitation laser beam and the gas mixture such that even for these relatively low rubidium densities a relative cooling of a macroscopic amount of gas can be observed when a sufficiently red-detuned excitation frequency for the excitation is chosen. This so-called redistributional laser cooling was first reported in Ref. [32], and is a result of the mean fluorescence of the rubidium atoms being shifted from the excitation frequencies, as the emission profile follows Kasha's rule due to the frequent collisions of the excited rubidium atoms with buffer-gas atoms during their electronic state lifetime. By excitation with a red-detuned laser beam this allows for the extraction of energy from the system, as described by [32]

$$\begin{aligned} P_{\text{cool}}(\nu_L) &= P_{\text{in}}(\nu_L)\alpha(\nu_L)\frac{\nu_{\text{fl}} - \nu_L}{\nu_{\text{fl}}} \\ &= P_{\text{abs}}(\nu_L)\frac{\nu_{\text{fl}} - \nu_L}{\nu_{\text{fl}}}. \end{aligned} \quad (3)$$

This expected cooling power is determined by the incoming beam power $P_{\text{in}}(\nu_L)$, the absorption coefficient for the particular excitation frequency $\alpha(\nu_L)$ (determining the interaction strength), and the detuning factor, which is a measure for the relative energy difference between the absorbed and the emitted photons. The detuning factor determines how much energy is extracted in one cooling cycle.

The resulting temperature change in the gas can be measured via the angular deflection of a second, off-resonant probe laser beam [a HeNe laser with a wavelength of 633 nm (473 THz), a power of 2 mW, and a beam diameter of 0.5 mm] for different relative distances to the excitation laser beam [for a sketch of the setup see Fig. 5(b)], as shown in Fig. 5(c) for three excitation frequencies. As described in Ref. [32] in more detail, the deflection results from the temperature change in the gas which in turn according to the corresponding local change of the gas density leads to a change in the refractive index and thereby to the deflection of the probe beam. The

polarity of this signal indicates whether the gas was heated up or cooled down during the cycles of excitation by the laser photons and the subsequent emission of frequency-shifted photons. As can be seen for the lowest-energetic excitation the deflection signal is flipped as the gas is cooled. Figure 5(d) shows corresponding data for the deflection normalized to the absorbed power [$P_{\text{abs}}(\nu_L) = P_{\text{in}}(\nu_L)\alpha(\nu_L)$] for three different cooling beam diameters, which within experimental accuracy follows the expected linear scaling. The observed magnitude of the slope reduces with increasing beam diameter, as can be understood from the smaller gradient of the imprinted temperature profile.

In a perfect system the change of sign in the deflection (which indicates the transition from heating to cooling) should take place when the excitation frequency becomes smaller than the mean fluorescence frequency, as then energy is extracted from the system. But, as pointed out already in Ref. [32], this only holds if no other effects, e.g., finite quantum efficiency, are present which can lead to energy being deposited in the system, counteracting the redistributional cooling. This would result in a shift of this crossover point towards smaller excitation frequencies, as indeed is visible in Fig. 5(d). As the observed crossover point shifts to lower frequencies for smaller beam diameters, it seems that loss processes depend nonlinearly on intensity, as could well be explained by excitation to higher-lying electronic rubidium states by energy pooling in the dense gas mixture [41,42].

VI. CONCLUSIONS

To conclude, we have reported absorption and emission spectroscopic measurements of rubidium atoms subject to helium-buffer-gas pressures up to 188-bar range at elevated temperatures. Spectra recorded in the presence of this light noble gas, which is of astrophysical relevance, show a Boltzmann-type Kennard-Stepanov frequency scaling between absorption and emission, thus extending measurements previously carried out in dense gas mixtures with heavier noble gases. Other than in the case of alkali-metal spectra recorded in the presence of the heavier argon noble gas, the

here observed spectral temperature is above the cell temperature. We have also reported spectroscopy and redistribution cooling measurements on rubidium–argon–gas mixtures at comparable temperature and pressure conditions, which extend earlier works on redistribution laser cooling. The here observed difference in spectral and thermodynamic temperature for the light-helium–buffer–gas–rubidium spectra hints at either incomplete thermalization of the quasimolecular manifold or a lower quantum efficiency than in the rubidium–argon system at comparable buffer-gas pressures. To characterize thermalization time scales for the present system as well as to identify potential loss or quenching channels, it would be interesting to do time-resolved studies of the spectra for different noble-gas–rubidium mixtures. For the future, it will also be interesting to test for evidence of possible thermalization effects of quasimolecular manifolds in the spectra of dense astrophysical objects. Laboratory experiments at

elevated pressure and temperature conditions, as required to allow for critical confrontations of spectroscopic theory with experimental studies of dense gases, demand technically challenging cell construction. Additionally, for future studies of redistribution laser cooling, it would be helpful to find spectroscopic samples that provide sufficient optical density at room-temperature conditions. Possible candidate systems are, e.g., mixtures containing acetylene or formaldehyde molecules, which have electronic transitions in the ultraviolet 200–300-nm wavelength regime accessible to frequency converted cw-laser sources, and a noble buffer gas.

ACKNOWLEDGMENTS

We acknowledge support from the Deutsche Forschungsgemeinschaft (Grants No. WE 1748-15 and No. 581412 and SFB/TR 185 Grant No. 277625399).

-
- [1] A. K. Pradhan and S. N. Nahar, *Atomic Astrophysics and Spectroscopy* (Cambridge University, New York, 2011).
- [2] S. Khalafinejad, C. von Essen, H. Hoeijmakers, G. Zhou, T. Klocová, J. Schmitt, S. Dreizler, M. Lopez-Morales, T.-O. Husser, T. Schmidt *et al.*, Exoplanetary atmospheric sodium revealed by orbital motion: Narrow-band transmission spectroscopy of HD 189733b with UVES, *Astron. Astrophys.* **598**, A131 (2017).
- [3] S. Harilal, B. Brumfield, N. LaHaye, K. Hartig, and M. Phillips, Optical spectroscopy of laser-produced plasmas for standoff isotopic analysis, *Appl. Phys. Rev.* **5**, 021301 (2018).
- [4] U. Vogl and M. Weitz, Spectroscopy of atomic rubidium at 500-bar buffer gas pressure: Approaching the thermal equilibrium of dressed atom-light states, *Phys. Rev. A* **78**, 011401(R) (2008).
- [5] P. Moroshkin, L. Weller, A. Saß, J. Klaers, and M. Weitz, Kennard-Stepanov Relation Connecting Absorption and Emission Spectra in an Atomic Gas, *Phys. Rev. Lett.* **113**, 063002 (2014).
- [6] S. Christopoulos, P. Moroshkin, L. Weller, B. Gerwers, R. Forge, T. Ockenfels, F. Vewinger, and M. Weitz, Rubidium spectroscopy at high-pressure buffer gas conditions: detailed balance in the optical interaction of an absorber coupled to a reservoir, *Phys. Scr.* **93**, 124006 (2018).
- [7] S.-y. Ch'en and M. Takeo, Broadening and shift of spectral lines due to the presence of foreign gases, *Rev. Mod. Phys.* **29**, 20 (1957).
- [8] A. G. Cameron, Abundances of the elements in the solar system, *Space Sci. Rev.* **15**, 121 (1973).
- [9] T. Ockenfels, F. Vewinger, and M. Weitz, Sapphire optical viewport for high pressure and temperature applications, *Rev. Sci. Instrum.* **92**, 065109 (2021).
- [10] J. R. Lakowicz, *Principles of Fluorescence Spectroscopy* (Springer, New York, 2013)
- [11] F. P. Schäfer, Principles of dye laser operation, *Dye Lasers* (Springer, Berlin, Heidelberg, 1973), pp. 1–85.
- [12] G. G. Stokes, On the change of refrangibility of light, *Phil. Trans. R. Soc. London* **142**, 463 (1852).
- [13] M. Kasha, Characterization of electronic transitions in complex molecules, *Discuss. Faraday Soc.* **9**, 14 (1950).
- [14] E. Kennard, On the thermodynamics of fluorescence, *Phys. Rev.* **11**, 29 (1918).
- [15] B. I. Stepanov, Universal relation between the absorption spectra and luminescence spectra of complex molecules, *Dokl. Akad. Nauk SSSR* **112**, 839 (1957).
- [16] T. Ihara, S. Maruyama, M. Yoshita, H. Akiyama, L. N. Pfeiffer, and K. W. West, Thermal-equilibrium relation between the optical emission and absorption spectra of a doped semiconductor quantum well, *Phys. Rev. B* **80**, 033307 (2009).
- [17] D. A. Sawicki and R. S. Knox, Universal relationship between optical emission and absorption of complex systems: An alternative approach, *Phys. Rev. A* **54**, 4837 (1996).
- [18] R. Croce, G. Zucchelli, F. M. Garlaschi, R. Bassi, and R. C. Jennings, Excited state equilibration in the photosystem I–light-harvesting I complex: P700 is almost isoenergetic with its antenna, *Biochemistry* **35**, 8572 (1996).
- [19] H. Dau and K. Sauer, Exciton equilibration and photosystem ii exciton dynamics: A fluorescence study on photosystem ii membrane particles of spinach, *Biochim. Biophys. Acta, Bioenerg.* **1273**, 175 (1996).
- [20] K. Dobek, The influence of temperature on coumarin 153 fluorescence kinetics, *J. Fluoresc.* **21**, 1547 (2011).
- [21] A. Kawski, P. Bojarski, and B. Kukliński, The local temperature dependence of fluorescent centres in pva films on the excitation wavenumber, *Z. Naturforsch. A* **55**, 653 (2000).
- [22] H. Kuhn and F. London, *London, Edinburgh, Dublin Philos. Mag. J. Sci.* **18**, 983 (1934).
- [23] H. Kuhn, XCIII. pressure shift and broadening of spectral lines, *London, Edinburgh, Dublin Philos. Mag. J. Sci.* **18**, 987 (1934).
- [24] H. Kuhn, Pressure shift of spectral lines, *Phys. Rev.* **52**, 133 (1937).
- [25] J. Franck and E. G. Dymond, Elementary processes of photochemical reactions, *Trans. Faraday Soc.* **21**, 536 (1926).
- [26] E. Condon, A theory of intensity distribution in band systems, *Phys. Rev.* **28**, 1182 (1926).
- [27] J. F. Kielkopf, Predicted alkali collision broadening by noble gases based on semiempirical potentials, *J. Phys. B* **9**, L547 (1976).
- [28] P. Anderson, A method of synthesis of the statistical and impact theories of pressure broadening, *Phys. Rev.* **86**, 809 (1952).

- [29] P. W. Anderson and J. D. Talman, Pressure broadening of spectral lines at general pressures, Bell Systems Technical Publication No. 3117 (1956).
- [30] J. Pascale, Use of l -dependent pseudopotentials in the study of alkali-metal-atom He systems: The adiabatic molecular potentials, *Phys. Rev. A* **28**, 632 (1983).
- [31] J. Dhiflaoui, H. Berriche, M. Herbane, A. Al Sehimi, and M. Heaven, Electronic structure and spectra of the rbar van der Waals system including spin-orbit interaction, *J. Phys. Chem. A* **116**, 10589 (2012).
- [32] U. Vogl and M. Weitz, Laser cooling by collisional redistribution of radiation, *Nature (London)* **461**, 70 (2009).
- [33] C. Ottinger, R. Scheps, G. York, and A. Gallagher, Broadening of the rb resonance lines by the noble gases, *Phys. Rev. A* **11**, 1815 (1975).
- [34] S.-Y. Ch'en, Broadening, asymmetry and shift of rubidium resonance lines under different pressures of helium and argon up to 100 atmospheres, *Phys. Rev.* **58**, 1051 (1940).
- [35] M. V. Romalis, E. Miron, and G. D. Cates, Pressure broadening of Rb D_1 and D_2 lines by ^3He , ^4He , N_2 , and Xe: Line cores and near wings, *Phys. Rev. A* **56**, 4569 (1997).
- [36] M. D. Rotondaro and G. P. Perram, Collisional broadening and shift of the rubidium D_1 and D_2 lines ($5^2 S_{1/2}$ $5^2 P_{1/2}$, $5^2 P_{3/2}$) by rare gases, H_2 , D_2 , N_2 , CH_4 and CF_4 , *J. Quant. Spectrosc. Radiat. Transfer* **57**, 497 (1997).
- [37] W. S. Miller, C. A. Rice, G. D. Hager, M. D. Rotondaro, H. Berriche, and G. P. Perram, High pressure line shapes of the Rb D_1 and D_2 lines for ^4He and ^3He collisions, *J. Quant. Spectrosc. Radiat. Transfer* **184**, 118 (2016).
- [38] F. Bouhadjar, K. Alioua, M. Bouazza, and M. Bouledroua, Rubidium D_1 and D_2 atomic lines pressure broadened by ground-state helium atoms, *J. Phys. B* **47**, 185201 (2014).
- [39] N. Allard and F. Spiegelman, Collisional line profiles of rubidium and cesium perturbed by helium and molecular hydrogen, *Astron. Astrophys.* **452**, 351 (2006).
- [40] C. A. Rice, K. Lapp, A. Rapp, W. S. Miller, and G. P. Perram, Rubidium D_1 and D_2 far wing line shapes induced by rare gases, *J. Quant. Spectrosc. Radiat. Transfer* **224**, 550 (2019).
- [41] S. Christopoulos, D. Möller, R. Cota, B. Gerwers, and M. Weitz, Verifying thermodynamic equilibrium of molecular manifolds: Kennard-Stepanov spectroscopy of a molecular gas, *Phys. Rev. A* **95**, 022510 (2017).
- [42] M. Allegrini, G. Alzetta, A. Kopystynska, L. Moi, and G. Orriols, Molecule formation and energy transfer processes in a vapor with high density of $3p$ -excited sodium atoms, *Opt. Commun.* **22**, 329 (1977).